REAL-TIME VALIDATION OF A SDR IMPLEMENTATION OF TDD WIMAX STANDARD

Ángel Carro-Lagoa (University of A Coruña, A Coruña, Spain; acarro@udc.es);
Pedro Suárez-Casal (University of A Coruña, A Coruña, Spain; pedro.scasal@udc.es);
Paula Fraga-Lamas (University of A Coruña, A Coruña, Spain; paula.fraga@udc.es);
José A. García-Naya (University of A Coruña, A Coruña, Spain; jagarcia@udc.es);
Luis Castedo (University of A Coruña, A Coruña, Spain; luis@udc.es);
Antonio Morales-Méndez (Indra Sistemas S.A., Aranjuez, Spain; ammendez@indra.es)

ABSTRACT

This paper focuses on the validation of an innovative software-defined radio architecture for a WiMAX system based on commercially available field-programmable gate array and digital signal processor modules. We provide a real-time implementation of a standard-compliant time-division duplex physical layer including a mobile and a base station as well as downlink and uplink communications, thus obtaining a full-featured physical layer. Additionally, a set of different configurations are supported as described in the standard and in the WiMAX Forum. The main contribution of the paper consists in a reproducible and repeatable validation of the implementation in representative scenarios. At the same time, a characterization of the performance exhibited by the system is provided based on bit error rate measurements carried out using a custom-made, real-time channel emulator.

1. INTRODUCTION

Worldwide Interoperability for Microwave Access (WiMAX) was initially conceived for wireless broadband access, but evolved with time until becoming a candidate technology for the so-called 4G mobile networks. In late 90s, IEEE started a working group to create a Point-to-Multi-Point (PMP) air interface that was proposed as an alternative to cable and digital subscriber line. The name was next coined by the WiMAX Forum, which was constituted to promote the interoperability of the standard. The original standard was modified as the IEEE 802.16d for fixed applications using Orthogonal Frequency-Division Multiplexing (OFDM) as the transmission scheme. In 2005, mobility support was incorporated based on Scalable Orthogonal Frequency-Division Multiple Access (SOFDMA), resulting in the amendment 802.16e also known as Mobile WiMAX. Four years later, the standard IEEE 802.16-2009 was released to support both fixed and mobile wireless communications. A complete survey of the historical evolution of the standard up to 2010 can be found in [1]. Recently, in 2011, WiMAX evolved to 802.16m [2], which focuses on providing an advanced air interface to fulfill the requirements of IMT-Advanced while maintaining backward compatibility with existing specifications. In August 2012, the IEEE 802.16-2012 [3] was released, consolidating material from IEEE 802.16j-2009 for relay-based networks and the amendment 802.16h-2010, which implements coexistence enhancement for license-exempt operation. Such a standard also incorporated the IEEE 802.16m-2011, but excluding the WirelessMAN Advanced Air Interface, which is now specified in the IEEE 802.16.1-2012 [4]. Finally, improvements focused on machine-to-machine applications are examined in amendments 802.16p-2012 [5] and 802.16.1b-2012 [6].

The physical layer is in charge of multiplexing user and system data together with control signaling in order to ensure a proper utilization of the radio resources. The design of the physical layer specifies how to map and how to allocate those resources as either reference signals or to form various physical channels. WiMAX supports several physical layer modes. Among them, OFDMA is the most appealing given its flexibility and ability to support multiple users at the same time.

WiMAX specifies both Frequency-Division Duplex (FDD) as well as Time-Division Duplex (TDD) operating modes. The election of TDD was based on its capabilities for dealing with the asymmetrical uplink/downlink data flow. In this way, one of the incentives of the present work is the scarcity of complete, real-time, OFDMA-TDD, mobile physical layer implementations available in the literature. Existing works focus on performance analysis such as path-loss measurements using Fixed WiMAX commercial equipment in rural environments [7], tests in outdoor scenarios employing commercial Mobile WiMAX equipment [8], or evaluations of the IEEE 802.16e OFDMA downlink in vehicular environments (ITU-R M.1225) [9]. In this context, simulations [10], non-real-time deployments [11, 12], and Fixed WiMAX implementations [13] are found. However, none of the aforementioned approaches accounts for software constraints or hardware limitations.

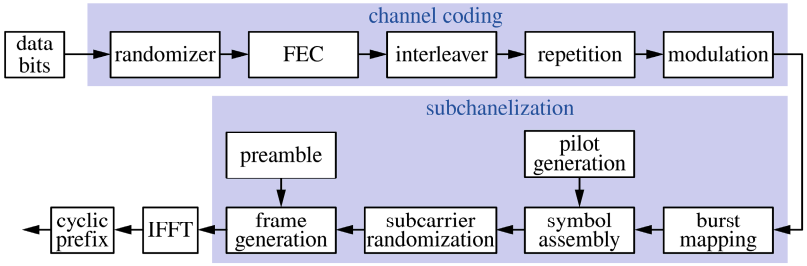

Figure 1: IEEE 802.16 transmitter block diagram.

The experimental validation of prototype baseband systems employing real-time hardware demonstrators confronts several challenges to be taken into account. Among them, formidable design complexity, long development time, high costs and manpower, or dealing with unsurmountable hardware issues are highlighted. To the knowledge of the authors, although several papers can be found in the literature describing real-time implementation and validation of downlink [14] or uplink channels [15], no one has been found dealing with both at the same time. It is worth mentioning that Mobile WiMAX duplex communications in a system-on-chip platform can be found in [16].

The main contribution of this paper is to describe the performance evaluation of the OFDMA-TDD physical layer implementation by means of repeatable and reproducible performance measurements of the Mobile WiMAX system under realistic conditions, validating the system as well as showing the versatility of the design through a wide variety of configurations.

The remainder of this article is organized as follows. Section 2 provides a brief description of the Mobile WiMAX physical layer, followed by the definition of the proposed hardware architecture in Section 3. Section 4 details the hardware components and the mapping of the real-time tasks to the hardware resources. The amount of resources consumed by the implementation is also detailed. Section 5 addresses the validation of the system, which is carried out by means of performance measurements over ITU-R channel models generated by a custom-made channel emulator. Finally, Section 6 is devoted to the conclusions and future research directions.

2. MOBILE WIMAX PHYSICAL LAYER

Mobile WiMAX is based on the OFDMA physical layer defined in the IEEE 802.16e standard. It supports both TDD and FDD operation modes whilst allowing for variable bandwidth and a scalable number of subcarriers ranging from 128 to 2048. Furthermore, WiMAX Forum specifies five profiles for interoperability as shown in Table 1. Such profiles combine different FFT sizes, bandwidths, and sampling frequencies.

The block diagram of the transmitter defined in the IEEE 802.16e standard is shown in Fig. 1. In TDD, a frame

Table 1: Mobile WiMAX profiles.

WiMAX profile	channel bandwidth [MHz]	sampling frequency [MHz]	FFT size
1	3.5	4	512
2	5	5.6	512
3	7	8	1024
4	8.75	10	1024
5	10	11.2	1024

is divided into downlink and uplink subframes. The downlink subframe consists of a preamble followed by a Frame Control Header (FCH), DL-MAP, and UL-MAP messages. If an UL-MAP message is sent to describe the uplink structure, it must be included in the first burst defined in the DL-MAP.

Mapping of bursts on subframes can be done using different permutation schemes such as non-adjacent groupings with Partial Usage of Subcarriers (PUSC) or Full Usage of Subcarriers (FUSC). The smallest data allocation unit is the slot, which is used to specify the time-frequency regions for data in the bursts. The slot definition varies according to the subcarrier grouping scheme.

Uplink resources are shared among mobile stations and their management is centralized on the Base Station (BS), which decides the amount of slots to be assigned to each mobile station based on the Quality-of-Service (QoS) parameters and bandwidth requirements for each connection. Additionally, the so-called ranging regions can be defined in the uplink to allow subscriber stations to perform network entry or to improve uplink synchronization parameters.

Data and pilot subcarriers are scrambled before the Inverse Fast Fourier Transform (IFFT) followed by Cyclic Prefix (CP) insertion are applied (see Fig. 1). Notice that the length of the cyclic prefix can take one the following values: 1/4, 1/8, 1/16, and 1/32.

In the IEEE 802.16e-2005, the channel coding stage consists of the following steps: data randomization, channel coding, bit-interleaving, repetition coding, and symbol mapping. Data randomization is performed in both uplink and downlink employing the output of a maximum-length shift-register sequence initialized at the beginning of every FEC block. Such a FEC block consists of an intenger num-

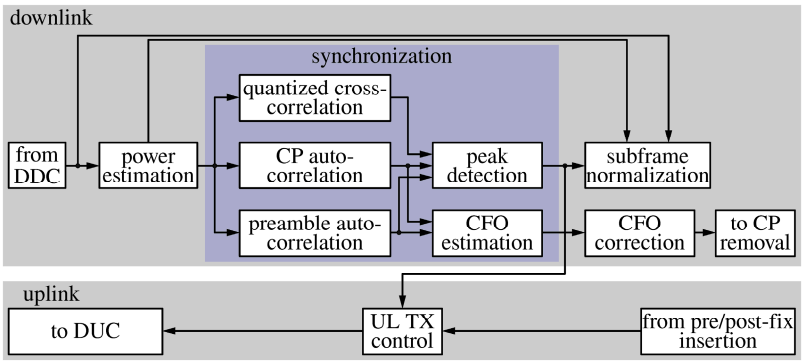

Figure 2: Downlink synchronization subsystem.

ber of subchannels. Channel coding is performed on a per-FEC-block basis employing one of the schemes defined in the standard, namely, Tail-Biting Convolutional Codes (TBCC), Block Turbo Codes (BTC), Convolutional Turbo Codes (CTC), and Low-Density Parity Check Codes (LDPC). Additionally, variable coding rate and modulation are supported, thus enabling for Adaptive Modulation and Coding (AMC) capabilities. Furthermore, Repetition coding with factors of 2, 4, or 6 are employed to increase the resilience of important control data. Finally, the modulation stage maps the coded bits into QPSK, 16-QAM, or 64-QAM constellations.

3. PROPOSED SYSTEM ARCHITECTURE

The real-time implementation described in this section focuses on the mandatory parts of the Mobile WiMAX physical layer for base and subscriber stations. It employs the OFDMA-TDD frame structure, PUSC permutation scheme both in the downlink and the uplink subframes, ranging, and channel coding based on TBCC.

3.1 Downlink Synchronization

Downlink synchronization consists of frame and symbol detection in the mobile station. Such tasks take advantage of the correlation properties exhibited by the preamble defined in the standard as well as those found in OFDM symbols when the cyclic prefix is included. The subsystem in charge of the downlink synchronization is shown in Fig. 2.

Preambles in Mobile WiMAX have a fixed structure with two guard subcarriers inserted between each pilot subcarrier and whose values are selected from a predefined set depending on the segment and base-station cell identifier. Frame detection is based on the Repetition Property Based (RPB) autocorrelation metric [17]. Next, two frequency offset estimations are obtained computing the angle of the previously declared autocorrelation values. The first one is extracted directly from the preamble, allowing for a wide frequency offset acquisition range. The second one is gathered from the cyclic prefixes, thus tracking the frequency offset on a per-OFDM-symbol basis.

3.2 Uplink Synchronization

Physical layers based on the OFDMA scheme require that uplink frames arrive at the base station at the same time and with a significant accuracy. This can only be achieved if all users are synchronized with the base station before the communication takes place. WiMAX standard states that the Round-Trip Delay (RTD) between the mobile station and the base station must be known beforehand by the mobile station, which is possible thanks to the so-called ranging.

For that purpose, mobile stations generate Pseudo Noise (PN) sequences from a shift register and they can be transmitted in specific regions of the uplink subframe. Such regions have to be reserved by the base station in a contention-based policy. At the receiver side (in the uplink), the base station detects the arrival of a ranging code, and then, it estimates the synchronization parameters. Finally, the mobile station adjusts its synchronization parameters from the base-station estimates sent back to the mobile station in a Medium Access Control (MAC) management message.

The standard defines different operation types depending on the current connection state: initial ranging on network entry, periodic ranging to update variations, bandwidth requests, and handover. During the initial ranging, OFDM symbols containing ranging codes are transmitted by the mobile station in pairs, the first one with a cyclic prefix, while the second one also adds a cyclic postfix, thus allowing for a wider time-synchronization margin.

Code detection and time-offset estimation at the base station takes place at the frequency domain over each received OFDM symbol. Firstly, a power threshold (see Fig. 2) followed by cross-correlation between the arriving subcarriers and all possible ranging codes is performed [18]. Once the ranging code is known, the received PN sequence is mapped back to the OFDM symbol. Since the initial rang-

ing forces mobile stations to transmit the same ranging code twice in two consecutive symbols, this property is exploited to extract the frequency offset through a correlation.

3.3 Subchannelization and Channel Equalization

Subchannelization involves interleaving and randomizing subcarriers followed by a permutation scheme and a pilot pattern. The base station specifies this structure for each frame using the dedicated DL-MAP and UL-MAP messages. Therefore, DL-MAP messages become critical since most of the processing of the downlink subframe at the receiver cannot start until this message has been completely decoded. On the other hand, subcarrier randomization in the uplink cannot be applied to the ranging bursts, thus this process depends entirely on the uplink burst scheme defined by the base station. We assign this task to the Digital Signal Processor (DSP) to provide the maximum flexibility with respect to the different sizes of the FFT, burst mapping, and eventual support of other permutation schemes (see Fig. 3).

Channel estimation and equalization is performed by inverting the pilot subcarriers and linearly interpolating the computed values for the remainder subcarriers.

3.4 Channel Coding

The proposed design supports a variable-rate TBCC coding scheme with constellation sizes varying from QPSK to 64-QAM both in downlink and uplink.

There are several techniques to design TBCC using standard convolutional encoders and Viterbi decoders [19]. The chosen technique offers a good trade-off between computational complexity and performance. The encoder is implemented adding a cyclic prefix to each FEC block with a size equal to the constraint length (in the case of WiMAX, such a value is set to 7). On the other hand, the decoder concatenates the first bits of the block at the end and vice versa, thus removing the additional bits from the decoder output.

The size of the chunks added at the beginning and at the end of the blocks is equal to the traceback length of the Viterbi decoder. If a block is shorter than the traceback length, it is just sent three times to the decoder and only the output corresponding to the second repetition is considered.

Additionally, the decoder computes a Carrier-to-Interference Noise Ratio (CINR) metric employing a soft decisor to estimate the transmitted symbols. It was verified that the algorithm provides accurate values of the CINR as long as decision errors are low. Otherwise, the CINR is overestimated.

Channel coding is mainly implemented in a Virtex II FPGA (see Fig. 3), although the optional repetition coding step performed over the constellation-mapped data and the processing control are both carried out in the DSP, using the FPGA as a coprocessor.

3.5 Physical Layer Control

Separation between MAC-level and physical-layer-level processing is obtained using the so-called OFDMA physical-layer Service Access Point (SAP) specification defined by Intel for its base stations [20]. Such a SAP provides the description of subframes, it sends and acquires data bursts, and it transmits and detects ranging codes.

The subframe structure is transferred to the mobile station through MAC management messages (DL-MAP, UL-MAP, Downlink Channel Descriptor (DCD), and Uplink Channel Descriptor (UCD)). Mobile WiMAX requires data bursts to be rectangular-shaped while spanning a multiple of two symbols in time and a multiple of a subchannel in frequency (the so-called slot unit). Although the standard allows for more than a single burst per mobile station, the corresponding DL-MAP overhead is increased. Moreover, the standard also allows for more than a single connection packed into a burst. Finally, the base station has to distribute the available resources between users, guaranteeing their QoS requirements.

Multiple burst-mapping proposals for Mobile WiMAX are presented in [21]. An approach suitable for the downlink is the so-called Ohseki algorithm [22], a reference algorithm considering complexity, requested bandwidth, and the shape of the downlink burst.

Resource management in the uplink is more flexible since it is only necessary to indicate the number of slots allocated to each station. The size of such allocations is decided by the MAC layer considering the QoS restrictions.

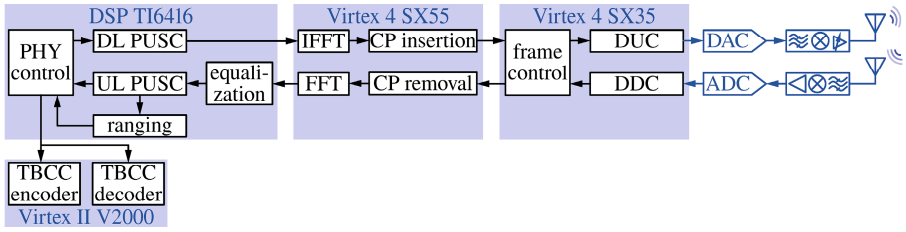

(a) Base station.

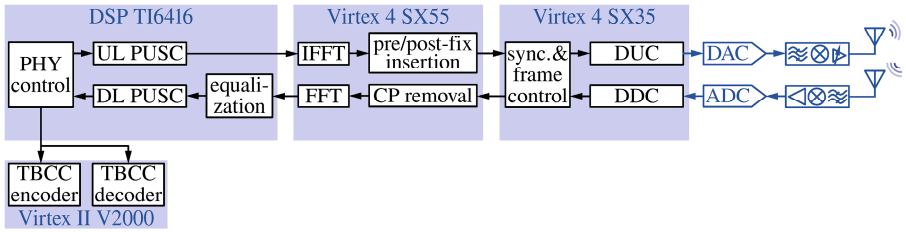

(b) Mobile station.

Figure 3: Hardware components and real-time software tasks with their allocation for the base station (a) and the mobile station (b).

4. HARDWARE DESCRIPTION

In the proposed design for a bi-directional TDD WiMAX system, mobile and base stations were implemented utilizing the same type of hardware elements based on Commercial Off-The-Shelf (COTS) components. An overview of the architecture defined for the base station and the mobile station is shown in Fig. 3. Each station consists of three different FPGAs and a DSP module placed on a Peripheral Component Interconnect (PCI) carrier board.

The first module contains a Texas Instruments TMS320C6416 DSP together with a Xilinx Virtex-II XC2V2000 FPGA. The second module has a Xilinx Virtex-4 XC4VSX55 FPGA, while the third one is equipped with a Virtex-4 XC4VSX35 FPGA together with an analog add-on module containing a dual Digital-to-Analog Converter (DAC) and a pair of Analog-to-Digital Converters (ADCs). Note that both Virtex-4 FPGAs are equipped with a large number of embedded multipliers, thus enabling intensive signal processing operations.

Data exchange between hardware modules is achieve using proprietary buses that can reach up to 400 MB/s, together with control-data buses limited to 20 MB/s. A PCI bus links the carrier board containing the hardware modules to a host computer.

In order to validate the real-time implementation as well as to assess the performance of the system, a channel emulator was implemented on a Xilinx Xtreme DSP Development Kit consisting of a Virtex-4 FPGA plus a couple of DACs and ADCs (see Fig. 4).

4.1 Digital Up/Down Conversion

Digital Up-Conversion (DUC) and Digital Down-Conversion (DDC) adapt the signals to the sampling rate of ADCs and DACs (see Fig. 3). In the case of the DUC, the following tasks are done: upsampling, pulse shaping, and I/Q modulation to a configurable intermediate frequency. The DDC performs the complementary operations in the reverse order. The chosen profiles selected by WiMAX Forum are supported providing five different bit-streams for the FPGAs. Each bit-stream has a different up/down-sampling factor. Since the DACs and the ADCs are configured with a sampling frequency of 80 MHz, the factors for each profile are respectively 20, 100/7, 10, 8, and 50/7 for profiles 1 to 5 (see Table 1). Each FPGA bit-stream also has a different optimized combination of interpolation/decimation filters in order to efficiently implement these sampling-rate conversions [23].

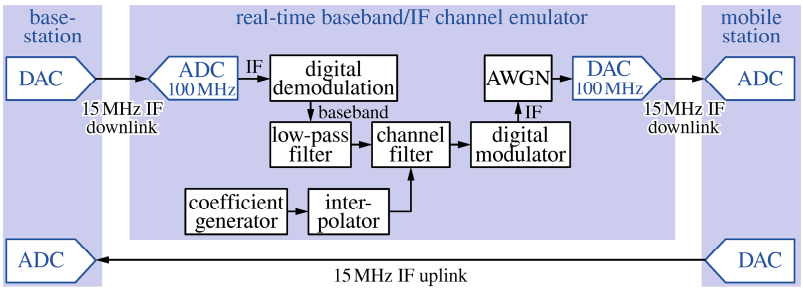

Figure 4: Real-time custom-made channel emulator utilized for validating the implementation.

Table 2: Resource utilization of the base station FPGAs.

base station	Virtex-II	Virtex-4 SX55	Virtex-4 SX35
Slice	10131/10752 (94%)	13785/24576 (56%)	6580/15360 (41%)
LUT	13509/21504 (62%)	18356/49152 (37%)	8261/30720 (26%)
RAMB16	52/56 (92%)	113/320 (35%)	45/192 (23%)
Multi-pliers	2/56 (3%)	116/512 (22%)	24/192 (12%)

Table 3: Resource utilization of the mobile station FPGAs.

mobile station	Virtex-II	Virtex-4 SX55	Virtex-4 SX35
Slice	10131/10752 (94%)	14692/24576 (59%)	15358/15360 (99%)
LUT	13509/21504 (62%)	19951/49152 (40%)	22625/30720 (73%)
RAMB16	52/56 (92%)	114/320 (35%)	52/192 (27%)
Multi-pliers	2/56 (3%)	117/512 (22%)	70/192 (36%)

4.2 Resource Utilization

FPGA designs were implemented using the Xilinx System Generator and built with Xilinx ISE 10.1. The resource utilization of the FPGAs is shown considering Slices, LUTs, RAMB16s, and multipliers for both base station (see Table 2) and mobile station (see Table 3).

The relatively high consumption of FPGA resources is explained because all FPGA tasks were implemented using the System Generator high-level development tool. Therefore, the implementation process becomes easier and faster, but the price to be paid is a non-optimum code in terms of resource utilization.

On the other hand, the higher resource utilization at the mobile station is because first, the synchronization block – which requires 68% of the slices available at the Virtex-4 SX35–, and second, the concatenation of cyclic postfixes at the IFFT output.

Table 4: Specification of the ITU-R M.1225 channel models employed in the performance evaluation.

	Pedestrian A	Pedestrian B	Vehicular A
Number of paths	4	6	6
Power of each path [dB]	0, –9.7, –19.2, –22.8	0, –0.9, –4.9, –8.0, –7.8, –23.9	0, –1.0, –9.0, –10.0, –15.0, –20.0
Path delay [ns]	0, 110, 190, 410	0, 200, 800, 1200, 2300, 3700	0, 310, 710, 1090, 1730, 2510
Speed [km/h]	3	3	60, 120

The utilization of a large FPGA as the Virtex-4 SX55 allows for a pipelined architecture dedicated to the FFT implementation. In case of the Virtex-II, an optimized FEC design was required due to the limited resources available.

Finally, apart from subchannelization, channel estimation and equalization, subcarrier mapping, and ranging (only at the base station); the SAP protocol, the minimum functionalities from the MAC required for the bi-directional operation, and data exchange with the host are all carried out by the DSP, thus demanding for a significant amount of resources from the DSP.

5. PERFORMANCE EVALUATION

This section describes the performance evaluation of the developed bi-directional TDD WiMAX physical layer. A diagram of the employed setup is shown in Fig. 4. For evaluating the downlink in a repeatable and in a reproducible fashion, the corresponding downlink subframes are transmitted across the channel emulator, whilst the uplink is connected with a cable. The reverse configuration is considere for evaluating the uplink.

The custom-made, real-time channel emulator was configured following the WiMAX Forum recommendations. Therefore, ITU-R M.1225 Pedestrian A at 3 km/h, Pedestrian B at 3 km/h, Vehicular A at 60 and at 120 km/h were considered assuming the tapped delay line characteristics summarized in Table 4. Notice that frequency selectivity

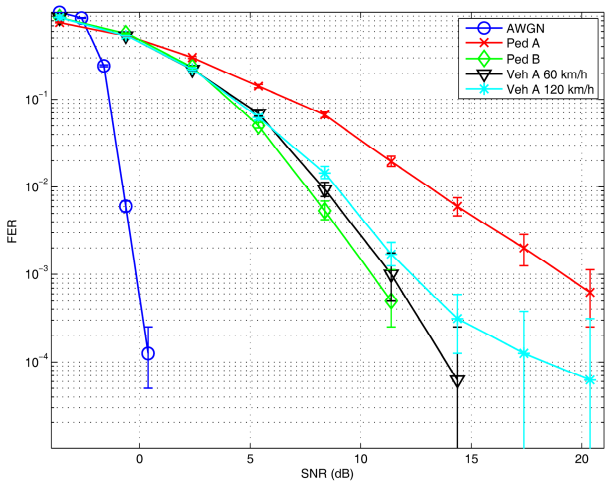

Figure 5: Downlink subframe detection in AWGN and ITU-R channels expressed in terms of FER with respect to the SNR.

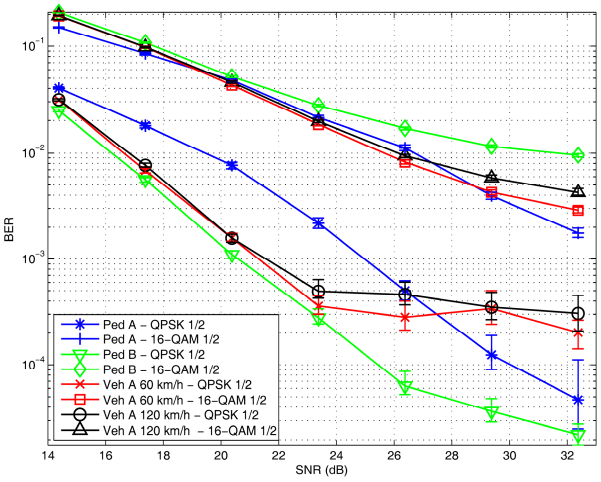

Figure 7: BER over ITU-R channels using the 8.5 MHz downlink profile.

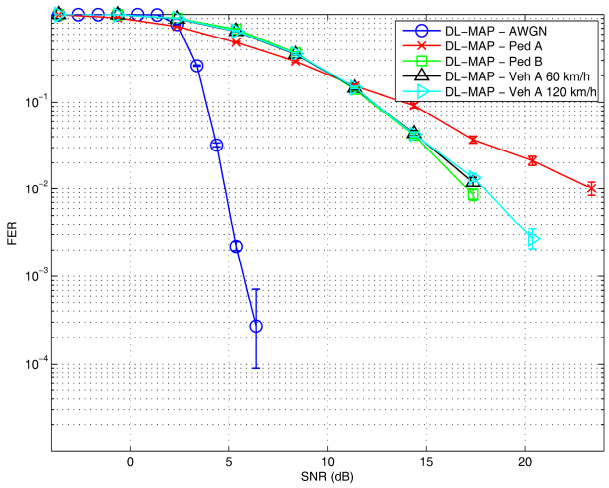

Figure 6: DL-MAP FER in AWGN and ITU-R channels.

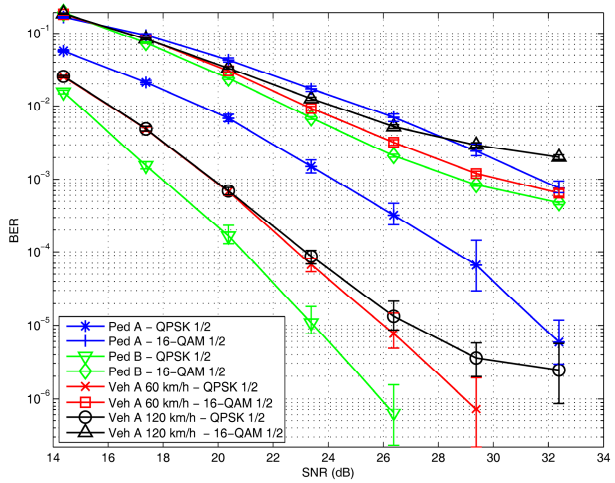

Figure 8: BER over ITU-R channels using the 8.5 MHz uplink profile.

exhibited by Pedestrian A is very low, whereas Pedestrian B and Vehicular A models provide richer multipath diversity and higher path delay spread than Pedestrian A.

Doppler spread computation is performed based on the Jakes Doppler power spectrum density assuming transmissions at 2.4 GHz. Note also that the maximum channel delay (3700 ns) does not exceed in any case the default 1/8 cyclic prefix length (11.429 ns). Consequently, the system is immune to Inter-Symbol Interference (ISI).

In order to plot the figure of merit with respect to the SNR, the AWGN generator included in the channel emulator is calibrated to match the SNR estimation obtained during the synchronization process.

First, downlink frame detection is evaluated transmitting more than 10^4 frames and counting the number of them correctly detected at the mobile station. The performance over AWGN and ITU-R channel models is shown in Fig. 5. In order to provide a measure of the uncertainty of the results, all performance results include 90% confidence intervals for the mean computed using bootstrapping.

Figure 5 shows that the results for the AWGN channel clearly outperform those obtained for the ITU-R channel models, which is mainly due to the channel fading. Pedestrian B and Vehicular A present a similar behavior, achieving FER values of 10^{-3} with a SNR value of 12 dB. Pedestrian A exhibits the worst performance caused by its lower

multipath diversity, thus making the synchronization more difficult.

According to the WiMAX standard, downlink synchronization is acquired if DL-MAP messages are correctly decoded. Following this criterion, FER is obtained distinguishing between undetected frames and frames in which the FDH or the DL-MAP are not correctly decoded (see Fig. 6). DL-MAP messages were sent using QPSK, convolutional coding at a rate of 1/2 with no repetitions, and a size of 28 bytes including the header and the Cyclic Redundancy Check (CRC).

Comparing Figs. 5 and 6 we can conclude that the frame detection has no negative impact on the system performance since the SNR for incorrectly detecting a frame is 5 dB lower than that for misdetecting the DL-MAP.

Uplink time-offset synchronization module is evaluated by the mobile station sending ranging codes while the base station stores the computed estimations. Following this procedure, it can be shown that the time offset estimation in the uplink is not affected by the particularities of the channel models, thus being suitable for all of them.

BER measurements are carried out considering a known structure for the subframes in order to avoid the case in which FCH or the DL-MAP messages cannot be decoded correctly. Figure 7 presents the BER for the 8.75 MHz downlink profile when the ITU-R channel models are employed. The Pedestrian A presents consistent results with those obtained for frame detection (see Figs. 5 and 6). Once higher SNR levels are achieved, the Pedestrian A outperforms other channel models since its channel frequency response is easier to equalize.

BER measurements for the uplink transmission for the 8.75 MHz profile are shown in Fig. 8. An improvement with respect to the downlink transmission is observed. Although surprising in principle, this behavior is perfectly justified when comparing the pilot structure of the uplink and downlink subframes. The effect is especially outstanding in the case of the Pedestrian B channel model. Due to the limited coherence time of Vehicular A channel models, there is a channel estimation error causing the error floor observed in Figs. 7 and 8, corresponding to the downlink and the uplink, respectively.

6. CONCLUSION

In this paper we have proposed the design and implementation of a real-time, bi-directional TDD physical layer compliant with the Mobile WiMAX standard. We have detailed the utilized SDR hardware architecture consisting of commercial off-the-shelf modules based on FPGAs and DSPs for both mobile and base stations. We have described in detail most of the design decisions pursuing an efficient utilization of the FPGA resources.

The implementation is validated in a repeatable and in a reproducible way by means of performance measurements carried out with the help of a real-time, custom-made channel emulator. Such a channel emulator implements AWGN as well as Pedestrian A and B, and Vehicular A channel models recommended by the WiMAX Forum. First, we tested the suitability of our synchronization algorithms, ensuring that they do not limit the performance of the system. Secondly, BER measurements were carried out for both the uplink and the downlink for the 8.75 MHz profile. The measurement results confirm that the proposed implementation is suitable for the scenarios modeled with the aforementioned channel models.

Finally, future research will be devoted to adapt our designs to the recently proposed WirelessMAN-Advanced Air Interface included in the IEEE 802.16m.

ACKNOWLEDGEMENTS

This work has been partially supported by Indra Sistemas S.A. and the Spanish Ministry of Defence with the technical direction of PEC/ITM under grant DN8644-COINCIDENTE. The authors wish to thank J. M. Camas-Albar from Indra Sistemas S.A. for his help.

This work has been additionally funded by Xunta de Galicia, Ministerio de Ciencia e Innovación of Spain, and FEDER funds of the European Union under grants with numbers 10TIC003CT, 09TIC008105PR, TEC2010-19545-C04-01, and CSD2008-00010.

REFERENCES

[1] D. Pareit, B. Lannoo, I. Moerman, P. Demeester, “The History of WiMAX: A Complete Survey of the Evolution in Certication and Standardization for IEEE 802.16 and WiMAX”, IEEE Communications Surveys Tutorials.

[2] IEEE Standard for Local and metropolitan area networks Part 16: Air Interface for Broadband Wireless Access Systems Amendment 3: Advanced Air Interface, IEEE Std 802.16m-2011(Amendment to IEEE Std 802.16-2009).

[3] IEEE Standard for Air Interface for Broadband Wireless Access Systems, IEEE Std 802.16-2012 (Revision of IEEE Std 802.16-2009).

[4] IEEE Standard for WirelessMAN-Advanced Air Interface for Broadband Wireless Access Systems, IEEE Std 802.16.1-2012.

[5] IEEE Standard for Air Interface for Broadband Wireless Access Systems. Amendment 1: Enhancements to Support Machine-to-Machine Applications, IEEE Std 802.16p-2012 (Amendment to IEEE Std 802.16-2012).

[6] IEEE Standard for WirelessMAN-Advanced Air Interface for Broadband Wireless Access Systems Amendment 1: Enhancements to Support Machine-to-Machine Applications, IEEE Std 802.16.1b-2012 (Amendment to IEEE Std 802.16.1-2012).

[7] P. Imperatore, E. Salvadori, I. Chlamtac, “Path Loss Measurements at 3.5 GHz: A Trial Test WiMAX Based in Rural Environment”, 3rd International Conference on Testbeds and

Research Infrastructure for the Development of Networks and Communities, 2007. TridentCom 2007, 2007, pp. 1 - 8. doi:10.1109/TRIDENTCOM.2007.4444709.

[8] G. Zaggoulos, M. Tran, A. Nix, "Mobile WiMAX system performance - simulated versus experimental results", IEEE 19th International Symposium on Personal, Indoor and Mobile Radio Communications, 2008. PIMRC 2008, 2008, pp. 1 -5. doi:10.1109/PIMRC.2008.4699670.

[9] R. Colda, T. Palade, E. Pucchita, I. Vermecan, A. Moldovan, "Mobile WiMAX: System performance on a vehicular multipath channel", Proceedings of the Fourth European Conference on Antennas and Propagation (EuCAP), 2010, 2010, pp. 1 - 5.

[10] Z. F. Mohamed M.A., M. R.H., "Simulation of WiMAX Physical Layer: IEEE 802.16e", IJCSNS International Journal of Computer Science and Network Security 10 (11).

[11] S. Hu, G. Wu, Y. L. Guan, C. L. Law, Y. Yan, S. Li, "Development and performance evaluation of mobile WiMAX testbed", IEEE Mobile WiMAX Symposium, 2007., 2007, pp. 104 -107. doi:10.1109/WIMAX.2007.348688.

[12] C. Mehlführer, S. Caban, M. Rupp, "Experimental Evaluation of Adaptive Modulation and Coding in MIMO WiMAX with Limited Feedback", EURASIP Journal on Advances in Signal Processing 2008, Article ID 837102.

[13] H. Lai, S. Boumaiza, "WiMAX baseband processor implementation and validation on a FPGA/DSP platform", Canadian Conference on Electrical and Computer Engineering, 2008. CCECE 2008, 2008, pp. 001449-001452. doi:10.1109/CCECE.2008.4564781.

[14] K.-C. Chang, J.-W. Lin, T.-D. Chiueh, "Design of a downlink baseband receiver for IEEE 802.16E OFDMA mode in high mobility", IEEE International SOC Conference, 2007, 2007, pp. 301-304. doi:10.1109/SOCC.2007.4545479.

[15] Y.-J. Wu, J.-M. Lin, H.-Y. Yu, H.-P. Ma, "A baseband testbed for uplink mobile MIMO WiMAX communications", IEEE International Symposium on Circuits and Systems, 2009. ISCAS 2009, 2009, pp. 794-797. doi: 10.1109/ISCAS.2009.5117874.

[16] G. Chuang, P.-A. Ting, J.-Y. Hsu, J.-Y. Lai, S.-C. Lo, Y.-C.Hsiao, T.-D. Chiueh, "A MIMO WiMAX SoC in 90nm CMOS for 300km/h mobility", IEEE International Solid-State Circuits Conference Digest of Technical Papers (ISSCC), 2011, 2011, pp. 134-136. doi:10.1109/ISSCC.2011.5746252.

[17] H. Kang, S.-B. Im, H.-J. Choi, D.-J. Rhee, "Robust OFDMA Frame Synchronization Algorithm on Inter-Cell Interference", Communications, 2006. APCC '06. Asia-Pacific Conference on, 2006, pp. 1-5.doi:10.1109/APCC.2006.255832.

[18] H. Mahmoud, H. Arslan, M. Ozdemir, "Initial Ranging for WiMAX (802.16e) OFDMA", IEEE Military Communications Conference, 2006. MILCOM 2006, 2006, pp. 1 -7. doi:10.1109/MILCOM.2006.302240.

[19] R. Cox, C. Sundberg, "An efficient adaptive circular Viterbi algorithm for decoding generalized tailbiting convolutional codes", IEEE Transactions on Vehicular Technology 43 (1) (1994) 57 -68. doi:10.1109/25.282266.

[20] OFDMA PHY SAP Interface Speccation for 802.16 Broadband Wireless Access Base Stations, Tech. rep., Intel Corporation (2007).

[21] C. So-In, R. Jain, A.-K. Tamimi, "Scheduling in IEEE 802.16e Mobile WiMAX Networks: Key Issues and a Survey", IEEE Journal on Selected Areas in Communications 27 (2) (2009) 156 -171. doi:10.1109/JSAC.2009.090207.

[22] T. Ohseki, M. Morita, T. Inoue, "Burst Construction and Packet Mapping Scheme for OFDMA Downlinks in IEEE 802.16 Systems", IEEE Global Telecommunications Conference, 2007. GLOBECOM '07, 2007, pp. 4307-4311. doi:10.1109/GLOCOM.2007.819.

[23] P. Suárez-Casal, A. Carro-Lagoa, J. García-Naya, L. Castedo, "A Multicore SDR Architecture for Reconfigurable WiMAX Downlink", 13th Euromicro Conference on Digital System Design: Architectures, Methods and Tools (DSD), 2010, 2010, pp. 801-804.doi:10.1109/DSD.2010.108.